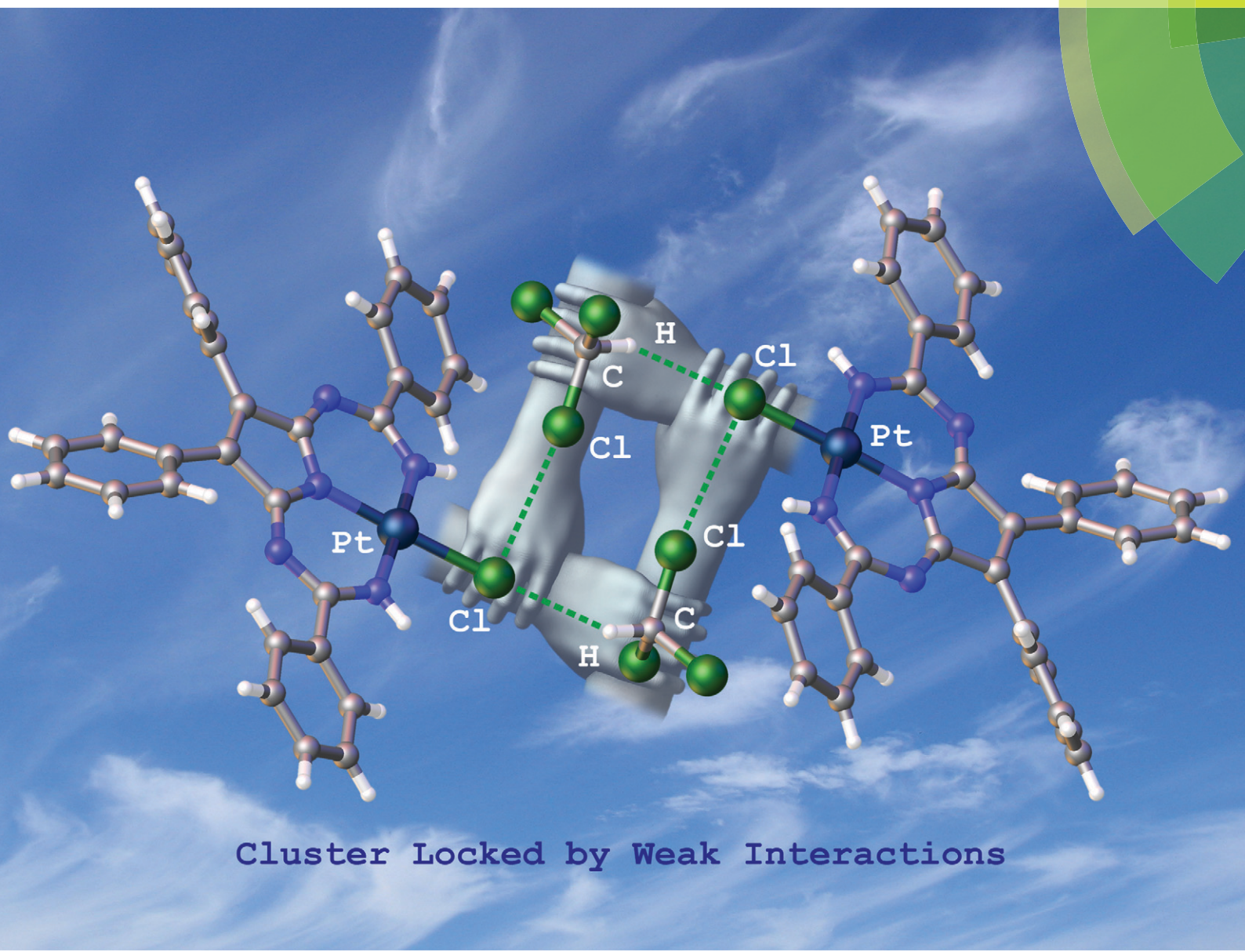


# CrystEngComm

[www.rsc.org/crystengcomm](http://www.rsc.org/crystengcomm)



Cluster Locked by Weak Interactions



PAPER

Vadim Yu. Kukushkin *et al.*

A family of heterotetrameric clusters of chloride species and halomethanes held by two halogen and two hydrogen bonds

175  
YEARS



Cite this: *CrystEngComm*, 2016, 18, 5278

## A family of heterotetrameric clusters of chloride species and halomethanes held by two halogen and two hydrogen bonds†

Daniil M. Ivanov,<sup>a</sup> Alexander S. Novikov,<sup>a</sup> Galina L. Starova,<sup>a</sup> Matti Haukka<sup>b</sup> and Vadim Yu. Kukushkin<sup>\*a</sup>

Two previously reported 1,3,5,7,9-pentaazanona-1,3,6,8-tetraenate (PANT) chloride platinum(II) complexes  $[\text{PtCl}(\text{HN}=\text{C}(\text{R})\text{N}=\text{CN}(\text{C}(\text{Ph})=\text{C}(\text{Ph})\text{C}=\text{NC}(\text{R})=\text{NH})]$  ( $\text{R} = {^t\text{Bu}}$  1, Ph 2) form solvates with halomethanes  $1\text{-}1\text{:CH}_2\text{Cl}_2$ ,  $1\text{-}1\text{:CH}_2\text{Br}_2$ , and  $2\text{-CHCl}_3$ . All these species feature novel complex-solvent heterotetrameric clusters, where the structural units are linked simultaneously by two  $\text{C}-\text{X}\cdots\text{Cl}-\text{Pt}$  ( $\text{X} = \text{Cl}, \text{Br}$ ) halogen and two  $\text{C}-\text{H}\cdots\text{Cl}-\text{Pt}$  hydrogen bonds. The geometric parameters of these weak interactions were determined using single-crystal XRD, and the natures of the XBs and HBs in the clusters were studied for the isolated model systems  $(1)_2\text{-}(\text{CH}_2\text{Cl}_2)_2$ ,  $(1)_2\text{-}(\text{CH}_2\text{Br}_2)_2$ , and  $(2)_2\text{-}(\text{CHCl}_3)_2$  using DFT calculations and Bader's AIM analysis. The evaluated energies of the weak interactions are in the range  $0.9\text{--}3.0 \text{ kcal mol}^{-1}$ . The XBs and HBs in the reported clusters are cooperative. In the cases of  $(1)_2\text{-}(\text{CH}_2\text{Cl}_2)_2$  and  $(1)_2\text{-}(\text{CH}_2\text{Br}_2)_2$ , the contribution of the HBs to the stabilization of the system is dominant, whereas for  $(2)_2\text{-}(\text{CHCl}_3)_2$  contributions of both types of the non-covalent interactions are almost the same. Crystal packing and other forces such as, e.g. dipole-dipole interactions, also affect the formation of the clusters.

Received 20th May 2016,  
Accepted 10th June 2016

DOI: 10.1039/c6ce01179a

[www.rsc.org/crystengcomm](http://www.rsc.org/crystengcomm)

### Introduction

Halogen bonds (XBs) are extremely important in crystal engineering and various type of XB have been intensively studied in recent years.<sup>1–4</sup> The XB is applied in pharmaceutical chemistry insofar as biologically active species featuring halide substituents can be co-crystallized with many organic and inorganic fragments forming XBs.<sup>5</sup> The recent applications of XBs include the stabilization of energetic materials (e.g. explosives) in the solid state<sup>6</sup> and the molecular design of materials with tunable photophysical properties.<sup>7</sup>

A XB is commonly treated as an electrostatic attraction between electron-rich centers and areas of electropositive potential, the so-called  $\sigma$ -holes, existing on the surfaces of covalently bonded halogen atoms.<sup>1–4,8–11</sup> The electron-rich centers can be heteroatoms such as halogens or  $\pi$ -systems. Two types of short halogen–halogen contact are usually discussed in the literature (Fig. 1).<sup>1,3,12</sup> Type I is believed to depend on the ef-

fects of close packing, whereas type II is due to a classic XB because a halogen atom with a  $90^\circ$  angle provides its lone pair for interaction and the other one provides its  $\sigma$ -hole. The type II interactions are more useful in crystal engineering due to the relatively strict geometrical requirements, whereas both angles around the halogen atoms in the type I interaction (which is actually not a XB, see ref. 13) can be in a wide range from  $180^\circ$  to  $90^\circ$  and less, and it hardly allows the construction of supramolecular structures.

Although the vast majority of XB studies involve metal-free organic species,<sup>1,2,14</sup> utilization of some organometallic compounds for these purposes are also reported.<sup>15,16</sup> The combination of unique redox, magnetic, and optical properties of metal complexes with adjustable organic moieties is very useful for the design of new materials.

XBs involving metal complexes form networks,<sup>16</sup> where anions are XB donors and their counterions are XB acceptors.

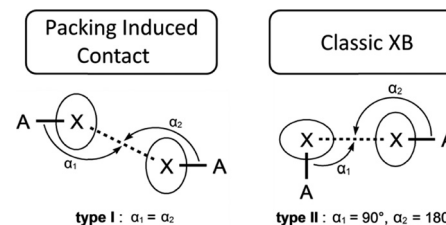


Fig. 1 Two types of halogen–halogen short contact.

<sup>a</sup> Institute of Chemistry, Saint Petersburg State University, 7/9 Universitetskaya Nab., 199034 Saint Petersburg, Russian Federation. E-mail: v.kukushkin@spbu.ru

<sup>b</sup> Department of Chemistry, University of Jyväskylä, P.O. Box 35, FI-40014

Jyväskylä, Finland

† Electronic supplementary information (ESI) available: Packing features of investigated solvates, description of other weak interactions, additional information for the theoretical consideration, full information for CCDC inspection, and cartesian atomic coordinates of the calculated equilibrium structures. CCDC 1456075, 1456509 and 1470271. For ESI and crystallographic data in CIF or other electronic format see DOI: 10.1039/c6ce01179a



These networks were found in halogen-containing pyridinium halometallates or cyanometallates ( $XC_5H_5-N_2[MX'_4]$  (where M is a divalent metal ion, *e.g.*,  $Co^{II}$ ,  $Pt^{II}$ , or  $Pd^{II}$ , X is a halogen except F, and X' is a halide or cyanide ligand).<sup>16–18</sup> Similar networks<sup>19,20</sup> have also been found in the associations of substituted ammonium bromometallates ( $^nPr_4N[CuBr_2]$ , ( $^nBu_4N)_2[MBr_4]$  (M = Zn, Cd, Co), and ( $^nBu_4N)_2[Pt_2Br_6]$  with bromoform, tetrabromomethane, and 1,1-dibromo-1,1,2,2-tetrafluoroethane serving as XB donors. 3D-Networks formed by XBs were also observed in the associations of ( $^nBu_4N)_2[PtBr_4Cl_2]$  and ( $^nBu_4N)_2[Pt_2Br_{10}]$  with dibromine.<sup>21</sup> Another large group of hybrid systems<sup>22,23</sup> is represented by complexes *trans*-[MX<sub>2</sub>(4-Xpy)<sub>2</sub>] forming intermolecular XBs between the halide ligands X<sup>–</sup> and halogen substituents X' in the pyridine ligands. In addition, palladium NCN<sup>24</sup> and PCP<sup>25</sup> pincer complexes featuring halide ligands were co-crystallized with diiodine, 1,4-diiodotetrafluorobenzene, and 1,4-diiodooctafluorobutane displaying networks and chains formed by XBs.

In most reports focused on crystal engineering involving XBs, strong iodine centered XB donors were explored, which contain the large  $\sigma$ -holes due to electron withdrawing substituents.<sup>1,3</sup> In contrast to a substantial number of these works, a few reports<sup>20,26–28</sup> have shown that even simple halomethanes can be effectively used in the design of structures held by XBs. In particular, we reported<sup>26</sup> that chloroform can act as both a XB and hydrogen bond (HB) donor forming the heterotetrameric clusters  $(Cl^-)_2 \cdot (CHCl_3)_2$  (Fig. 2) in the solid state. The term “heterotetrameric cluster” means a symmetrical supramolecular associate formed by two pairs of different species (dimer of a dimer). This term was previously suggested for designation of neutral clusters with halomethanes containing four molecules linked by two HBs and two XBs.<sup>27,28</sup>

In this study, we demonstrate that relevant heterotetrameric structures could be obtained using crystallization of the annulated triazapentadiene systems, *viz.* 1,3,5,7,9-pentaazanona-1,3,6,8-tetraenate (PANT) platinum(II) chloride complexes (Fig. 3, A), with the halomethanes  $CH_2Cl_2$ ,  $CH_2Br_2$ , and  $CHCl_3$  (Fig. 3, B). The heterotetramers display the previously unreported  $H_2ClC-Cl \cdots Cl-Pt$ ,  $H_2BrC-Br \cdots Cl-Pt$ , and  $HCl_2C-Cl \cdots Cl-Pt$  halogen and the C–H $\cdots$ Cl–Pt hydrogen bonds. These experimental data along with the results of a detailed inspection of the large amount of available litera-

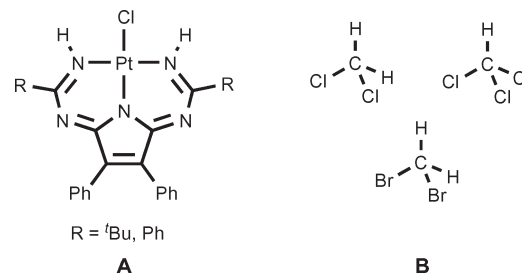


Fig. 3 Structures of the  $[PtCl(PANT)]$  complexes (A) and the halomethanes (B) employed in this work.

ture/CCDC data open up a new family of heterotetrameric clusters held simultaneously by two C–X $\cdots$ Cl XBs and two C–H $\cdots$ Cl HBs with halomethanes. All our results are discussed in the sections that follow.

## Results and discussion

### Synthesis and crystallization

In accordance with our recently reported procedure,<sup>29</sup> the PANT platinum(II) chloride complexes were synthesized by coupling of the nitrile ligands in *trans*-[PtCl<sub>2</sub>(RCN)<sub>2</sub>] with 2,3-diphenylmaleimide (molar ratio 1 : 2.5,  $CH_2Cl_2$ , RT) followed by purification of the formed  $[PtCl(PANT)]$  complexes using column chromatography.

Two PANT species ( $R = ^nBu$  1,  $Ph$  2) were found to co-crystallize with halomethanes ( $CHCl_3$ ,  $CH_2Cl_2$ , and  $CH_2Br_2$ ) forming heterotetrameric complex-halomethane clusters (Table 1). Isostructural Cl/Br exchange was detected for clusters 1 with  $CH_2Cl_2$  and  $CH_2Br_2$  and corresponding crystalline phases demonstrate close cell parameters and analogous packing features (for detailed information see ESI†).

### The C–X $\cdots$ Cl–Pt halogen bonds

In general, a C–X $\cdots$ Cl–Pt (X = Cl, Br) XB occurs when the distance between the appropriate X atoms is less than the sum of their van der Waals (vdW) radii. However, one should take into consideration that several data sets for vdW radii based on different approaches have been suggested for the same atoms/ions and the Cl and Br vdW radii vary from 1.75 to 1.80 Å and from 1.85 to 1.90 Å, respectively, depending on the system used. Currently the most widely used vdW radii system was proposed by Bondi<sup>30</sup> with the smallest values so far suggested. It is commonly accepted that X atoms are involved in non-covalent interactions when the X $\cdots$ X distance is shorter than the sum of the Bondi's vdW radii. However, it has also been argued that Bondi's vdW radii are too small by a systematic deviation and too close to the corresponding

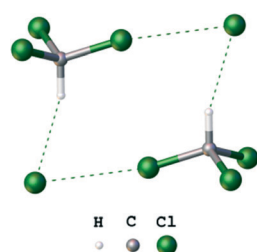


Fig. 2 Ball-and-stick model of the heterotetrameric cluster  $(Cl^-)_2 \cdot (CHCl_3)_2$ .<sup>26</sup>

Table 1 Numbering of complexes and solvates

| R      | Nos | Solvent system | Solvates                     |
|--------|-----|----------------|------------------------------|
| $^nBu$ | 1   | $CH_2Cl_2$     | $1 \cdot 1 \cdot 4 CH_2Cl_2$ |
|        |     | $CH_2Br_2$     | $1 \cdot 1 \cdot 4 CH_2Br_2$ |
| Ph     | 2   | $CHCl_3$       | $2 \cdot CHCl_3$             |



covalent radii.<sup>31</sup> A possible alternative for the Bondi's vDW radii is the data set proposed by Rowland,<sup>32</sup> which was obtained by inspection of a large amount of statistical data, and it is believed that Rowland's values fit better for the investigation of HBs<sup>33</sup> and XB<sup>34</sup> in the solid phase and in calculated model systems<sup>35</sup> and we used these radii for the analysis of the obtained experimental data.

The C–X···Cl–Pt (X = Cl, Br) short contacts (3.447(2) Å and 3.5012(9) for Cl···Cl, and 3.330(2) for Cl···Br) that are less than the sum of Rowland's<sup>32</sup> vDW radii ( $2R_w(\text{Cl}) = 3.52$  Å,  $R_w(\text{Cl}) + R_w(\text{Br}) = 3.63$  Å) were found in each cluster (Table 2). The corresponding angles around the chloride ligands are close to 90° and around solvent halogen atoms are close to 180°. These data indicate that the short contacts are due to the XB and complex molecules behave as XB acceptors of type II (Fig. 1).

Solvates  $1\cdot1\text{H}_2\text{CH}_2\text{Cl}_2$ ,  $1\cdot1\text{H}_2\text{CH}_2\text{Br}_2$  (Fig. 4), and  $2\cdot\text{CHCl}_3$  (Fig. 5) form independent heterotetrameric clusters comprised of two solvent molecules and two molecules of the complexes linked by two XB and two hydrogen bonds (HBs). In 1, the geometric parameters of these heterotetramers are very similar. Structures  $1\cdot\text{CH}_2\text{Br}_2$  and  $2\cdot\text{CHCl}_3$  demonstrate the first examples of the  $\text{H}_2\text{BrC–Br}\cdots\text{Cl–Pt}$  and the  $\text{HCl}_2\text{C–Cl}\cdots\text{Cl–Pt}$  XB<sub>s</sub>, and only the  $\text{H}_2\text{ClC–Cl}\cdots\text{Cl–Pt}$  contact was previously observed.<sup>36</sup>

### Theoretical consideration of the XB<sub>s</sub> and HBs in the heterotetrameric clusters

Analysis of the crystallographic data shows that the clusters exhibit short contacts, which may be caused by non-covalent interactions such as HBs and XB<sub>s</sub> and/or by the crystal packing effects. In addition, a significant limitation of the X-ray crystallography is the impossibility of determining the exact positions of light atoms (first of all hydrogen atoms) and this greatly complicates the interpretation of experimental information. In order to clarify the situation, we carried out theoretical DFT calculations so that the nature of the weak interactions can be analyzed in detail by using computational methods.

We focused on the study of isolated heterotetrameric clusters from  $1\cdot1\text{H}_2\text{CH}_2\text{Cl}_2$ ,  $1\cdot1\text{H}_2\text{CH}_2\text{Br}_2$ , and  $2\cdot\text{CHCl}_3$  (Fig. 6, struc-

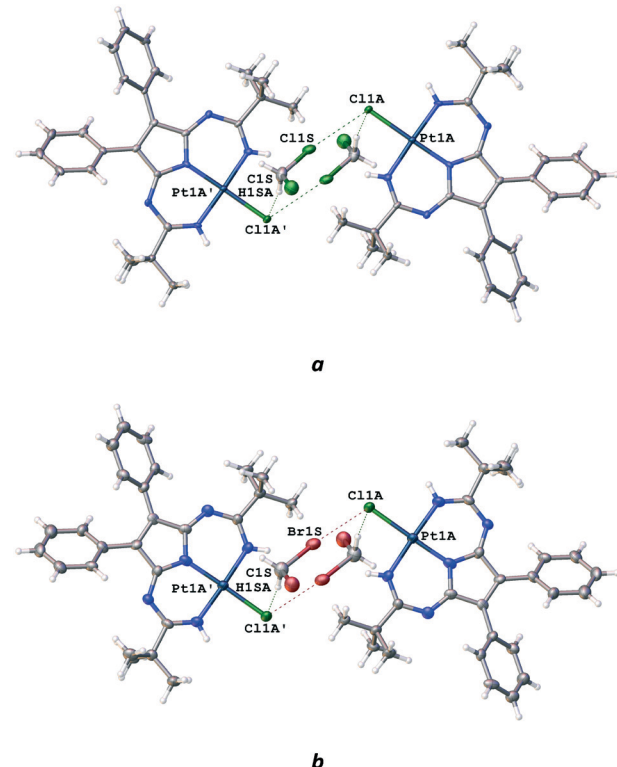


Fig. 4 The halogen and hydrogen bonds in the isostructural heterotetramers from  $1\cdot1\text{H}_2\text{CH}_2\text{Cl}_2$  (a) and  $1\cdot1\text{H}_2\text{CH}_2\text{Br}_2$  (b). Thermal ellipsoids are shown with 50% probability.

tures  $(1)_2\cdot(\text{CH}_2\text{Cl}_2)_2$ ,  $(1)_2\cdot(\text{CH}_2\text{Br}_2)_2$ , and  $(2)_2\cdot(\text{CHCl}_3)_2$ , respectively) taking into account that if the crystal packing effects are significant, the structures should change substantially on going from the solid state to the gas phase during the geometry optimization procedure. Otherwise the geometries expectedly are preserved in the isolated form.<sup>37</sup>

This commonly accepted approach helps to exclude the crystal packing effects from consideration and to investigate the short contacts only within the clusters.

The results of our theoretical calculations are summarized in Tables 2, 3 and S5.† In the case of  $(1)_2\cdot(\text{CH}_2\text{Cl}_2)_2$ , we found an asymmetric distortion of the structure and the emergence of two new short contacts N–H···Cl–CH<sub>2</sub>Cl. Both  $\text{HCl}_2\text{C–}$

Table 2 The characteristic parameters of the C–X···Cl–Pt halogen bonds in the experimental (plain text) and theoretically optimized (italics) clusters as well as the energies of these bonds  $E_b$  (kcal mol<sup>−1</sup>) determined using two methods (for details see ESI, Table S5)

| Cluster                                | Pt–Cl···X–C          | $d(\text{X}\cdots\text{Cl})$ , Å | $\angle(\text{C–X}\cdots\text{Cl})$ , ° | $\angle(\text{C}\cdots\text{Cl–Pt})$ , ° | $E_b^a$ | $E_b^b$ |
|--|----------------------|----------------------------------|---|--|---------|---------|
| $(1)_2\cdot(\text{CH}_2\text{Cl}_2)_2$ | C1S–Cl1S···Cl1A–Pt1A | 3.447(2)                         | 171.8(3)                                | 108.41(7)                                |         |         |
|  |                      | 3.50                             | 168.4                                   | 109.9                                    | 0.9     | 1.4     |
|  |                      | 3.36                             | 170.8                                   | 108.9                                    | 1.6     | 1.6     |
| $(1)_2\cdot(\text{CH}_2\text{Br}_2)_2$ | C1S–Cl1S···Cl1A–Pt1A | 3.330(2)                         | 172.0(4)                                | 107.98(8)                                |         |         |
|  |                      | 3.17                             | 171.0                                   | 106.2                                    | 2.5     | 2.7     |
|  |                      | 3.61                             | 172.16(7)                               | 87.902(17)                               |         |         |
| $(2)_2\cdot(\text{CHCl}_3)_2$          | C1S–Cl3S···Cl1–Pt1   | 3.5012(9)                        | 169.7                                   | 83.8                                     | 0.9     | 1.1     |
|  |                      | 3.61                             | 180                                     | 90                                       |         |         |
| *Comparison <sup>c</sup>               |                      | 3.52 (Cl···Cl)<br>3.63 (Cl···Br) |   |  |         |         |

<sup>a</sup>  $E_b = -V(r)/2$ .<sup>38</sup> <sup>b</sup>  $E_b = 0.429G(r)$ .<sup>39</sup> <sup>c</sup> Comparison between the sum of Rowland's<sup>32</sup> vDW radii and conventional halogen bond angle.



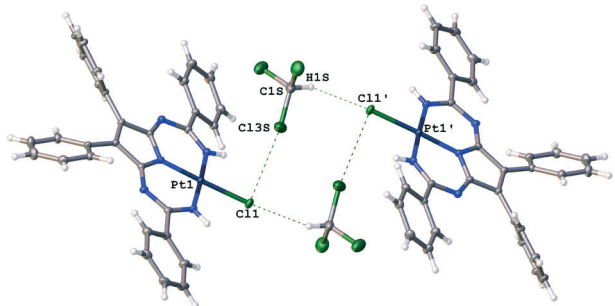


Fig. 5 The halogen and hydrogen bonds in the heterotetramer from 2-CHCl<sub>3</sub>. Thermal ellipsoids are shown with 50% probability.

H···Cl-Pt contacts are shortened (by 0.19 and 0.11 Å) one of the H<sub>2</sub>ClC-Cl···Cl-Pt contacts is very slightly elongated (by 0.05 Å), and another one is slightly shortened (by 0.09 Å). In the case of (1)<sub>2</sub>·(CH<sub>2</sub>Br<sub>2</sub>)<sub>2</sub>, the symmetrical structure of the cluster is preserved and both the HBr<sub>2</sub>C-H···Cl-Pt contacts are significantly elongated (by 0.51 Å), two new short contacts N-H···Br-CH<sub>2</sub>Br are formed, and the H<sub>2</sub>BrC-Br···Cl-Pt contacts are shortened (by 0.16 Å).

For (2)<sub>2</sub>·(CHCl<sub>3</sub>)<sub>2</sub>, both Cl<sub>3</sub>C-H···Cl-Pt contacts are shortened (by 0.31 Å) and the HCl<sub>2</sub>C-Cl···Cl-Pt contacts are slightly elongated (by 0.11 Å) on going from the solid state to the gas phase, whereas the length of the HCl<sub>2</sub>C-Cl···Ph contacts remains virtually unchanged. In all three cases, the  $\angle$ (C-X···Cl) and  $\angle$ (X···Cl-Pt) angles (X = Cl, Br) are changed insignificantly and the largest deviation from the experimental values (4°) was observed in the case of the  $\angle$ (Cl···Cl-Pt) angle in (2)<sub>2</sub>·(CHCl<sub>3</sub>)<sub>2</sub>.

Additional information on the nature of the short contacts in (1)<sub>2</sub>·(CH<sub>2</sub>Cl<sub>2</sub>)<sub>2</sub>, (1)<sub>2</sub>·(CH<sub>2</sub>Br<sub>2</sub>)<sub>2</sub>, and (2)<sub>2</sub>·(CHCl<sub>3</sub>)<sub>2</sub>, can be obtained using the topological analysis of the electron density distribution (AIM method).<sup>40</sup> This approach has already been successfully used by us upon studies of non-covalent interactions and properties of coordination bonds in various transition metal complexes and organic compounds.<sup>37,41-46</sup> The low magnitude of the electron density and the positive values of the Laplacian and energy density in appropriate bond critical points (3, -1) (Table S5†) are typical for XBs<sup>47-50</sup> and also for some HBs<sup>51</sup> indicating that the interaction is weak.<sup>52,53</sup> We have defined the energies of these contacts according to the procedures proposed by Espinosa *et al.*<sup>38</sup> and Vener *et al.*<sup>39</sup> (1-3 kcal mol<sup>-1</sup>), and one can state that these bonds may be classified as very weak mainly due to the electrostatic and dispersion interactions. The strength of the XBs decreases in the series: (1)<sub>2</sub>·(CH<sub>2</sub>Br<sub>2</sub>)<sub>2</sub> > (1)<sub>2</sub>·(CH<sub>2</sub>Cl<sub>2</sub>)<sub>2</sub> > (2)<sub>2</sub>·(CHCl<sub>3</sub>)<sub>2</sub>. Bond critical points (3, -1) for very long HBr<sub>2</sub>C-H···Cl-Pt contacts in (1)<sub>2</sub>·(CH<sub>2</sub>Br<sub>2</sub>)<sub>2</sub> were not found.

We evaluated the vertical total energies of the heterotetrameric clusters dissociation ( $E_v$ ) through the “halogen” and “hydrogen” contacts for (1)<sub>2</sub>·(CH<sub>2</sub>Cl<sub>2</sub>)<sub>2</sub>, (1)<sub>2</sub>·(CH<sub>2</sub>Br<sub>2</sub>)<sub>2</sub>, and (2)<sub>2</sub>·(CHCl<sub>3</sub>)<sub>2</sub>; corresponding values of  $E_v$  are given in Table 4. The cooperativity of the XBs and HBs was recognized for the studied heterotetramers. Thus, to quantify the relative contributions of these non-covalent interactions in the stabilization of the heterotetrameric clusters, we calculated the vertical total energies of their dissociation ( $E_v$ ) through the “halogen” and “hydrogen” contacts for (1)<sub>2</sub>·(CH<sub>2</sub>Cl<sub>2</sub>)<sub>2</sub>, (1)<sub>2</sub>·(CH<sub>2</sub>Br<sub>2</sub>)<sub>2</sub>, and (2)<sub>2</sub>·(CHCl<sub>3</sub>)<sub>2</sub>, the corresponding values of  $E_v$  are given in Table 4. For (1)<sub>2</sub>·(CH<sub>2</sub>Cl<sub>2</sub>)<sub>2</sub> the contribution of the HBs to the stabilization of the system prevail nearly twice over the contribution of XBs, for (1)<sub>2</sub>·(CH<sub>2</sub>Br<sub>2</sub>)<sub>2</sub> – approximately by one third, and for (2)<sub>2</sub>·(CHCl<sub>3</sub>)<sub>2</sub> contributions of both types of non-covalent interaction are almost the same. The existence of (1)<sub>2</sub>·(CH<sub>2</sub>Cl<sub>2</sub>)<sub>2</sub> and (1)<sub>2</sub>·(CH<sub>2</sub>Br<sub>2</sub>)<sub>2</sub> is determined mainly by HBs, whereas for (2)<sub>2</sub>·(CHCl<sub>3</sub>)<sub>2</sub> both types of non-covalent interaction are equally essential. In the case of (2)<sub>2</sub>·(CHCl<sub>3</sub>)<sub>2</sub>, the non-covalent interactions make the major contribution to

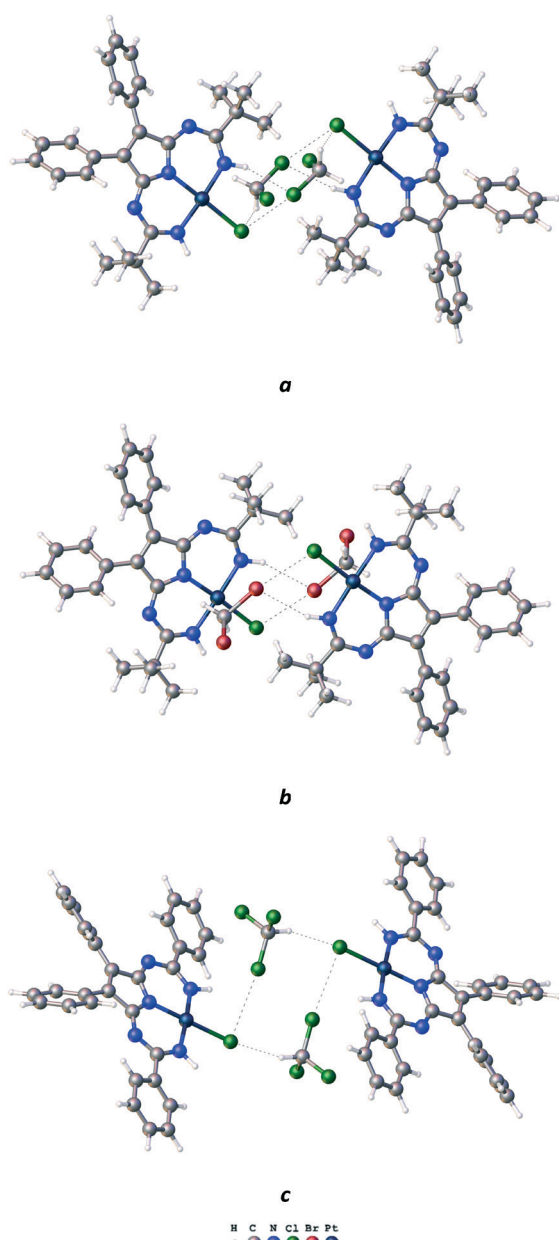


Fig. 6 Views of the optimized heterotetrameric clusters (1)<sub>2</sub>·(CH<sub>2</sub>Cl<sub>2</sub>)<sub>2</sub> (a), (1)<sub>2</sub>·(CH<sub>2</sub>Br<sub>2</sub>)<sub>2</sub> (b), and (2)<sub>2</sub>·(CHCl<sub>3</sub>)<sub>2</sub> (c).



**Table 3** The characteristic parameters of the C–H···Cl–Pt hydrogen bonds in the experimental (plain text) and theoretically optimized (italics) clusters as well as the energies of these bonds  $E_b$  (kcal mol<sup>-1</sup>) determined using two methods (for details see ESI, Table S5)

| Cluster                                  | C–H···Cl                 | $d(\text{Cl} \cdots \text{H})$ , Å | $d(\text{Cl} \cdots \text{C})$ , Å | $\angle(\text{C–H} \cdots \text{Cl})$ , ° | $E_b^a$ | $E_b^b$ |
|--|--------------------------|------------------------------------|------------------------------------|---|---------|---------|
| $(1)_2 \cdot (\text{CH}_2\text{Cl}_2)_2$ | C1S–H1SA···Cl1A'         | 2.809                              | 3.708(8)                           | 154.6                                     | 2.2     | 2.4     |
|  |                          | 2.63                               | 3.595                              | 147.316                                   |         |         |
|  |                          | 2.70                               | 3.666                              | 147.033                                   |         |         |
| $(1)_2 \cdot (\text{CH}_2\text{Br}_2)_2$ | C1S–H1SB···Cl1A'         | 2.786                              | 3.696(12)                          | 156.5                                     | 1.9     | 1.9     |
|  |                          | 3.304                              | 4.211                              | 141.279                                   |         |         |
|  |                          | 2.795                              | 3.4989(17)                         | 127.8                                     |         |         |
| $(2)_2 \cdot (\text{CHCl}_3)_2$          | C1S–H1S···Cl1'           | 2.476                              | 3.410                              | 142.624                                   | 2.8     | 3.0     |
|  |                          | 2.86                               | 3.53                               | 120                                       |         |         |
|  | *Comparison <sup>c</sup> |                                    |                                    |   |         |         |

<sup>a</sup>  $E_b = -V(r)/2$ .<sup>38</sup> <sup>b</sup>  $E_b = 0.429G(r)$ .<sup>39</sup> <sup>c</sup> Comparison between the sum of Rowland's<sup>32</sup> vdW radii and the minimal hydrogen bond angle.

the stabilization of the cluster, whereas for  $(1)_2 \cdot (\text{CH}_2\text{Cl}_2)_2$  and especially for  $(1)_2 \cdot (\text{CH}_2\text{Br}_2)_2$  the role of the XB and HBs in stabilization of these supramolecular systems is, although smaller, still quite significant.

Thus, the results of our theoretical calculations reveal that the crystal packing noticeably affects the geometrical features of the heterotetrameric clusters and also that the XB and HBs in these supramolecular associates are relatively weak.

The formation of such ordered structures as the heterotetramers can be accompanied by a significant entropy decrease and stabilization of the system from the energy viewpoint. In order to prove that, we tried to carry out a geometry optimization procedure for the two model metal-free systems, *viz.* the “heterotetramer” and the “heterotrimer plus one outlying chloroform molecule”,  $(\text{Cl}^-)_2 \cdot (\text{CHCl}_3)_2$  and  $(\text{Cl}^-)_2 \cdot (\text{CHCl}_3) + \text{CHCl}_3$ , respectively (M06-2X/6-311++G(d,p) level of theory). We located the minima for the heterotetramer  $(\text{Cl}^-)_2 \cdot (\text{CHCl}_3)_2$  (Fig. 7) on the potential energy surface. However, several attempts to find an appropriate stationary point for the  $(\text{Cl}^-)_2 \cdot (\text{CHCl}_3) + \text{CHCl}_3$  system with the outlying chloroform molecule led to the separation of this model system into two fragments  $\text{Cl}^- \cdot (\text{CHCl}_3)$ , which move away from each other upon the geometry optimization (Fig. 8); we finished the optimization when the distance between these fragments exceeded 13 Å. A possible rationale for this phenomenon is an electrostatic repulsion between the two chloride anions. In conjunction with the found minima for the heterotetrameric system  $(\text{Cl}^-)_2 \cdot (\text{CHCl}_3)_2$ , our results suggest that the presence of two  $\text{Cl}^-$  close to each other in the crystal lattice can be provided through the formation of bridges with  $\text{CHCl}_3$ . These neutral species sufficiently shield the negatively

charged anions thus providing their coexistence in the close proximity.

#### Retrieved CCDC data for the heterotetrameric clusters

The heterotetrameric clusters stabilized simultaneously by two C–X···Cl XB and two C–X···Cl–R HBs (Fig. 9) were not described in the literature except for only one example  $(\text{Cl}^-)_2 \cdot (\text{CHCl}_3)_2$  reported by us.<sup>25</sup> Therefore we inspected available CCDC data for these heterotetrameric clusters to clarify consistent patterns of their formation.

The first type of cluster is stabilized by two C–X···Cl–R XB and two C–X···Cl–R HBs (Fig. 9, cluster A) incorporating a neutral RCl species as the Lewis base. We also acquired data on analogous clusters where free chloride anions behave as both XB and HB acceptors (Fig. 9, cluster B). Noticeably, in each cluster the XB and HBs alternate with each other. Other variants of bridging molecules in the clusters with two HBs and two XBs were not found.

**Structures with dichloromethane and chloroform.** We found 26 type A clusters (Fig. 9) with chloroform and 7 with dichloromethane. All of them, except the three clusters from structures QATCOF, QOWGOY, and XESTAS, have a center of symmetry. Structure XESTAS has an axis of symmetry, because it contains chiral molecules of the complex. All these type A clusters were not discussed in the corresponding articles, although HBs were mentioned for structures FOLJOH,<sup>54</sup> JUGCUX,<sup>55</sup> UBIFIU,<sup>56</sup> and DCLMET11 (ref. 57) and XB were noted for UBIFIU<sup>56</sup> and DCLMET11.<sup>57</sup> In most cases, chloride

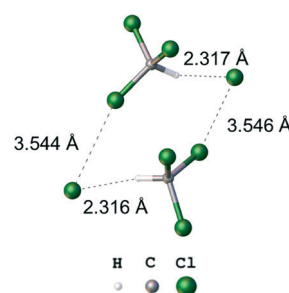


Fig. 7 Calculated cluster  $(\text{Cl}^-)_2 \cdot (\text{CHCl}_3)_2$ .

**Table 4** Vertical total energies of heterotetrameric clusters dissociation ( $E_v$ ) in kcal mol<sup>-1</sup>

| Cluster                                  | Dissociation   | $E_v$ |
|--|----------------|-------|
| $(1)_2 \cdot (\text{CH}_2\text{Cl}_2)_2$ | Through the XB | 12.09 |
|  | Through the HB | 21.58 |
| $(1)_2 \cdot (\text{CH}_2\text{Br}_2)_2$ | Through the XB | 30.77 |
|  | Through the HB | 38.88 |
| $(2)_2 \cdot (\text{CHCl}_3)_2$          | Through the XB | 8.94  |
|  | Through the HB | 8.26  |



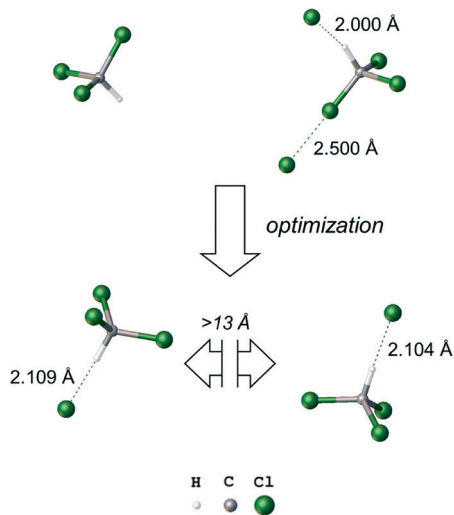


Fig. 8 Attempted calculation of  $(\text{Cl}^-)_2 \cdot (\text{CHCl}_3) + \text{CHCl}_3$ .

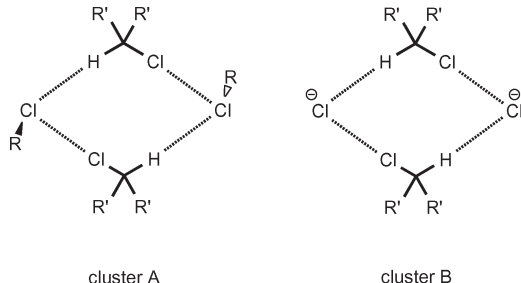


Fig. 9 Schematic representation of the heterotetrameric clusters with  $\text{R}-\text{Cl}$  (cluster A) or  $\text{Cl}^-$  (cluster B) as both the HB and XB acceptors and  $\text{R}_2\text{CHCl}$  as the XB and HB donors.

metal complexes ( $\text{R} = \text{ML}_n$ ) are both XB and HB acceptors, and only in structure DCLMET11 featuring the tetrameric fragment  $(\text{CH}_2\text{Cl}_2)_4$ , are the consequences of two HBs and two XBs found.

In the case of free chloride anions as both the HB and XB acceptors, 8 type B clusters (Fig. 9) with chloroform and 3 clusters with dichloromethane were found and all of them exhibited a center of symmetry. Only one cluster in structure UPEROX was described in our previous work.<sup>26</sup>

**Other structures.** Dibromomethane has been so rarely studied as an XB donor with only the  $\text{H}_2\text{BrC-Br}\cdots\text{Br}$ ,<sup>58,59</sup>  $\text{H}_2\text{BrC-Br}\cdots\text{O}$ ,<sup>60</sup> and  $\text{H}_2\text{BrC-Br}\cdots\text{N}$ <sup>61</sup> short contacts reported and the heterotetrameric clusters with bromine as a XB donor are unknown. However, one more tetrameric structure was found for 1,8,exo-9,10,11pentachloropentacyclo[6.2.1.1<sup>3,6</sup>.0<sup>2,7</sup>.0<sup>4,10</sup>]-dodecan-5-one (structure KAVDUG, Fig. 10). Thus, only two examples with  $\text{R} \neq \text{ML}_n$  were reported. Parameters of the weak interactions in the clusters and our criteria for the CCDC search are given in the ESI.<sup>†</sup>

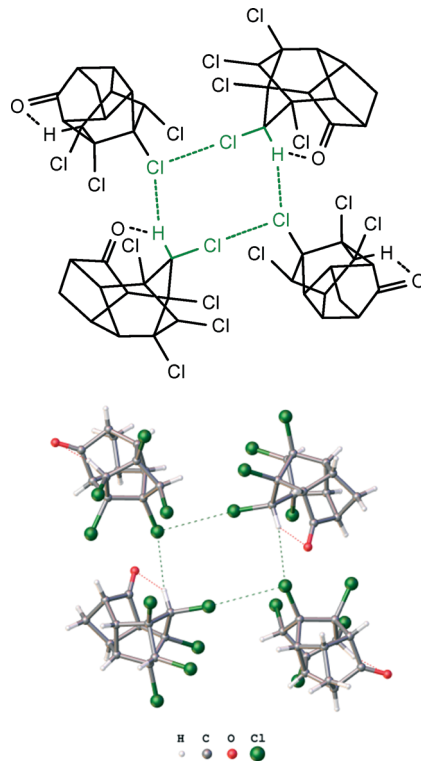


Fig. 10 ChemDraw (top) and ball-and-stick (bottom) models of the tetrameric cluster from KAVDUG.

## Experimental

### Crystallization and XRD experiments

Compounds **1** and **2** were synthesized as previously described.<sup>29</sup> Solvents were obtained from commercial sources and used as received. Crystals **1·1½CH<sub>2</sub>Cl<sub>2</sub>**, **1·1½CH<sub>2</sub>Br<sub>2</sub>**, and **2·CHCl<sub>3</sub>** were grown using the slow evaporation of **1** and **2** solutions in corresponding solvents.

A suitable crystal of **1·1½CH<sub>2</sub>Cl<sub>2</sub>** was studied on an Xcalibur, Eos diffractometer. The crystal was kept at 100(2) K during data collection. Using Olex2 1.2,<sup>58</sup> the structure was solved with the ShelXT<sup>59</sup> structure solution program using Direct Methods and refined with the ShelXL-2014 (ref. 60) refinement package using Least Squares minimisation.

A suitable crystal of **1·1½CH<sub>2</sub>Br<sub>2</sub>** was studied on a SuperNova, Dual, Cu at zero, Atlas diffractometer. The crystal was kept at 100(2) K during data collection. Using Olex2,<sup>58</sup> the structure was solved with the ShelXS<sup>60</sup> structure solution program using Direct Methods and refined with the ShelXL<sup>60</sup> refinement package using Least Squares minimisation. The unit cell of **1·1½CH<sub>2</sub>Br<sub>2</sub>** also contains disordered molecules of CH<sub>2</sub>Br<sub>2</sub> (total potential solvent accessible void volume is 305 Å<sup>3</sup>; electron count per cell is 206 electrons) that have been treated as a diffuse contribution to the overall scattering without specific atom positions using SQUEEZE/PLATON.<sup>61</sup>

A suitable crystal of **2·CHCl<sub>3</sub>** was immersed in cryo-oil, mounted in a Nylon loop, and measured at a temperature of 100 K. The X-ray diffraction data was collected on a Bruker

Smart Apex II diffractometer using Mo K $\alpha$  radiation ( $\lambda = 0.71073 \text{ \AA}$ ). The SAINT<sup>62</sup> programme package was used for cell refinement and data reduction. The structure was solved using direct methods using a SHELXS-97 (ref. 60) programme. A numerical absorption correction (SADABS)<sup>63</sup> was applied to the data. Structural refinements were carried out using SHELXL-97.<sup>60</sup>

### Computational details

The full geometry optimization of  $(1)_2 \cdot (\text{CH}_2\text{Cl}_2)_2$ ,  $(1)_2 \cdot (\text{CH}_2\text{Br}_2)_2$ , and  $(2)_2 \cdot (\text{CHCl}_3)_2$  has been carried out at the DFT theory level using the M06 functional<sup>64</sup> with the help of the Gaussian-09<sup>65</sup> program package. The experimental X-ray geometries were used as starting points for the theoretical geometry optimization procedure. The calculations were carried out using a quasi-relativistic Stuttgart pseudopotential that described 60 core electrons and the appropriate contracted basis set<sup>66</sup> for the platinum atoms and the 6-31G(d) basis set for other atoms. The M06 functional is much less time-consuming than the MP2 method used by us previously,<sup>26,67</sup> at the same time, the M06 functional describes reasonably weak dispersion forces and non-covalent interactions.<sup>68,69</sup> No symmetry operations have been applied. The Hessian matrix was calculated analytically to prove the location of the correct minima (no imaginary frequencies). The topological analysis of the electron density distribution with the help of the atoms in molecules (AIM) method developed by Bader<sup>40</sup> has been performed by using the Multiwfn program (version 3.3.4).<sup>70</sup>

## Conclusions

The results of this work could be considered from the following perspectives. Firstly, we report here on a new family of heterotetrameric clusters held simultaneously by two C-X $\cdots$ Cl XB and two C-H $\cdots$ Cl HBs with halomethanes. This family has now been extended from a single associate of  $\text{CHCl}_3$  with uncomplexed  $\text{Cl}^-$  (previously reported by us<sup>26</sup>) to a large set of heterotetramers incorporating (i) not only  $\text{CHCl}_3$ , but also rather weak XB/HB donors such as  $\text{CH}_2\text{Cl}_2$  and  $\text{CH}_2\text{Br}_2$ , (ii) neutral chloride platinum(II) complexes, where XB/HB-accepting chloride is bound to a platinum center, and (iii) organic molecules, RCl, acting as a simultaneous XB/HB donor and XB/HB acceptor. Secondly, our theoretical calculations indicate that the XBs and HBs in the reported clusters are cooperative. In the cases of  $(1)_2 \cdot (\text{CH}_2\text{Cl}_2)_2$  and  $(1)_2 \cdot (\text{CH}_2\text{Br}_2)_2$ , the contribution of the HBs to the stabilization of the system is dominant, whereas for  $(2)_2 \cdot (\text{CHCl}_3)_2$  the contributions of both types of non-covalent interaction are almost the same. Another theoretical study conducted in this work for the simple model systems,  $(\text{Cl}^-)_2 \cdot (\text{CHCl}_3)_2$  and  $(\text{Cl}^-)_2 \cdot (\text{CHCl}_3) + \text{CHCl}_3$ , gives an idea that the halomethane in the heterotetramers shields the chloride anions thus preventing their Coulomb repulsion and the destruction of these clusters. Thirdly, two clusters,  $(1)_2 \cdot (\text{CH}_2\text{Cl}_2)_2$  and  $(1)_2 \cdot (\text{CH}_2\text{Br}_2)_2$ , were found to be isostructural, which indicates a possibility

of the  $\text{CH}_2\text{Cl}_2/\text{CH}_2\text{Br}_2$  exchange with preservation of the geometrical parameters. Such isostructural exchange can be useful for the prediction of crystal structures and in the design of a series of clusters held using weak interactions and exhibiting close geometrical features. We expect that all these findings can find an application in crystal engineering and materials science, and we hope that our results open up an avenue to the generation of other similar heterotetramers and works in this direction are under way in our group.

## Acknowledgements

D. M. I. and A. S. N. are grateful to the Russian Foundation for Basic Research for the support of their studies (grant 16-33-00212). V. Y. K. thanks Saint Petersburg State University for research grant (12.38.225.2014). XRD studies were performed at the Center for X-ray Diffraction Studies (Saint Petersburg State University), whereas the structure determination of  $2 \cdot \text{CHCl}_3$  was performed at the University of Jyväskylä.

## Notes and references

- 1 A. Karpfen, A. C. Legon, W. T. Pennington, T. W. Hanks, H. D. Arman, P. Metrangolo, G. Resnati, T. Pilati, S. Biella, S. V. Rosokha, J. K. Kochi, D. W. Bruce and M. Fourmigüé, in *Halogen Bonding: Fundamentals and Applications*, ed. P. Metrangolo and G. Resnati, Springer-Verlag Berlin, Berlin, 2008, vol. 126, pp. 1–221.
- 2 G. Cavallo, P. Metrangolo, T. Pilati, G. Resnati, M. Sansotera and G. Terraneo, *Chem. Soc. Rev.*, 2010, **39**, 3772–3783.
- 3 A. Mukherjee, S. Tothadi and G. R. Desiraju, *Acc. Chem. Res.*, 2014, **47**, 2514–2524.
- 4 P. Politzer, J. S. Murray and T. Clark, *Phys. Chem. Chem. Phys.*, 2013, **15**, 11178–11189.
- 5 P. Auffinger, F. A. Hays, E. Westhof and P. S. Ho, *Proc. Natl. Acad. Sci. U. S. A.*, 2004, **101**, 16789–16794.
- 6 K. B. Landenberger, O. Bolton and A. J. Matzger, *J. Am. Chem. Soc.*, 2015, **137**, 5074–5079.
- 7 V. V. Sivchik, A. I. Solomatina, Y.-T. Chen, A. J. Karttunen, S. P. Tunik, P.-T. Chou and I. O. Koshevoy, *Angew. Chem., Int. Ed.*, 2015, **54**, 14057–14060.
- 8 G. Cavallo, P. Metrangolo, T. Pilati, G. Resnati and G. Terraneo, *Cryst. Growth Des.*, 2014, **14**, 2697–2702.
- 9 A. Bundhun, P. Ramasami, J. S. Murray and P. Politzer, *J. Mol. Model.*, 2013, **19**, 2739–2746.
- 10 T. Clark, M. Hennemann, J. S. Murray and P. Politzer, *J. Mol. Model.*, 2007, **13**, 291–296.
- 11 X. J. Mu, Q. T. Wang, L. P. Wang, S. D. Fried, J. P. Piquemal, K. N. Dalby and P. Y. Ren, *J. Phys. Chem. B*, 2014, **118**, 6456–6465.
- 12 F. F. Awwadi, R. D. Willett, K. A. Peterson and B. Twamley, *Chem. – Eur. J.*, 2006, **12**, 8952–8960.
- 13 P. Metrangolo and G. Resnati, *IUCrJ*, 2014, **1**, 5–7.
- 14 F. H. Allen, P. A. Wood and P. T. A. Galek, *Acta Crystallogr., Sect. B: Struct. Sci.*, 2013, **69**, 379–388.

15 L. Brammer, G. M. Espallargas and S. Libri, *CrystEngComm*, 2008, **10**, 1712–1727.

16 R. Bertani, P. Sgarbossa, A. Venzo, F. Lelj, M. Amati, G. Resnati, T. Pilati, P. Metrangolo and G. Terraneo, *Coord. Chem. Rev.*, 2010, **254**, 677–695.

17 G. M. Espallargas, L. Brammer and P. Sherwood, *Angew. Chem., Int. Ed.*, 2006, **45**, 435–440.

18 L. Brammer, G. M. Espallargas and H. Adams, *CrystEngComm*, 2003, **5**, 343–345.

19 S. V. Rosokha, J. Lu, T. Y. Rosokha and J. K. Kochi, *Chem. Commun.*, 2007, 3383–3385.

20 S. V. Rosokha and M. K. Vinakos, *Cryst. Growth Des.*, 2012, **12**, 4149–4156.

21 M. Berkei, J. F. Bickley, B. T. Heaton and A. Steiner, *Chem. Commun.*, 2002, 2180–2181.

22 F. Zordan, L. Brammer and P. Sherwood, *J. Am. Chem. Soc.*, 2005, **127**, 5979–5989.

23 G. M. Espallargas, F. Zordan, L. A. Marin, H. Adams, K. Shankland, J. van de Streek and L. Brammer, *Chem. – Eur. J.*, 2009, **15**, 7554–7568.

24 A. M. Mills, J. A. M. van Beek, G. van Koten and A. L. Spek, *Acta Crystallogr., Sect. C: Cryst. Struct. Commun.*, 2002, **58**, m304–m306.

25 M. T. Johnson, Z. Dzolic, M. Cetina, O. F. Wendt, L. Ohrstrom and K. Rissanen, *Cryst. Growth Des.*, 2012, **12**, 362–368.

26 P. V. Gushchin, G. L. Starova, M. Haukka, M. L. Kuznetsov, I. L. Eremenko and V. Y. Kukushkin, *Cryst. Growth Des.*, 2010, **10**, 4839–4846.

27 D. S. Yufit, O. V. Shishkin, R. I. Zubatyuk and J. A. K. Howard, *Cryst. Growth Des.*, 2014, **14**, 4303–4309.

28 D. S. Yufit, O. V. Shishkin, R. I. Zubatyuk and J. A. K. Howard, *Kristallografiya*, 2014, **229**, 639–647.

29 D. M. Ivanov, P. V. Gushchin, A. S. Novikov, M. S. Avdontceva, A. A. Zolotarev, G. L. Starova, Y.-T. Chen, S.-H. Liu, P.-T. Chou and V. Y. Kukushkin, *Eur. J. Inorg. Chem.*, 2016, **2016**, 1480–1487.

30 A. Bondi, *J. Phys. Chem.*, 1964, **68**, 441–451.

31 A. N. Chernyshev, M. V. Chernysheva, P. Hirva, V. Y. Kukushkin and M. Haukka, *Dalton Trans.*, 2015, **44**, 14523–14531.

32 R. S. Rowland and R. Taylor, *J. Phys. Chem.*, 1996, **100**, 7384–7391.

33 T. Steiner, *Angew. Chem., Int. Ed.*, 2002, **41**, 48–76.

34 L. C. Gilday, S. W. Robinson, T. A. Barendt, M. J. Langton, B. R. Mullaney and P. D. Beer, *Chem. Rev.*, 2015, **115**, 7118–7195.

35 J. Tomasi, B. Mennucci and R. Cammi, *Chem. Rev.*, 2005, **105**, 2999–3093.

36 J. Seo, I. Yoon, J. E. Lee, M. R. Song, S. Y. Lee, S. H. Park, T. H. Kim, K. M. Park, B. G. Kim and S. S. Lee, *Inorg. Chem. Commun.*, 2005, **8**, 916–919.

37 A. A. Melekhova, A. S. Novikov, K. V. Luzyanin, N. A. Bokach, G. L. Starova, V. V. Gurzhiy and V. Y. Kukushkin, *Inorg. Chim. Acta*, 2015, **434**, 31–36.

38 E. Espinosa, E. Molins and C. Lecomte, *Chem. Phys. Lett.*, 1998, **285**, 170–173.

39 M. V. Vener, A. N. Egorova, A. V. Churakov and V. G. J. Tsirelson, *Comput. Chem.*, 2012, **33**, 2303–2309.

40 R. F. W. Bader, *Atoms in Molecules: A Quantum Theory*, Oxford University Press, Oxford, 1990.

41 D. M. Ivanov, Y. V. Kirina, A. S. Novikov, G. L. Starova and V. Y. Kukushkin, *J. Mol. Struct.*, 2015, **1104**, 19–23.

42 X. Ding, M. J. Tuikka, P. Hirva, V. Y. Kukushkin, A. S. Novikov and M. Haukka, *CrystEngComm*, 2016, **18**, 1987–1995.

43 K. I. Kulish, A. S. Novikov, P. M. Tolstoy, D. S. Bolotin, N. A. Bokach, A. A. Zolotarev and V. Y. Kukushkin, *J. Mol. Struct.*, 2016, **1111**, 142–150.

44 A. S. Novikov, M. L. Kuznetsov and A. J. L. Pombeiro, *Chem. – Eur. J.*, 2013, **19**, 2874–2888.

45 A. S. Novikov and M. L. Kuznetsov, *Inorg. Chim. Acta*, 2012, **380**, 78–89.

46 D. M. Ivanov, A. S. Novikov, I. V. Ananyev, Y. V. Kirina and V. Y. Kukushkin, *Chem. Commun.*, 2016, **52**, 5565–5568.

47 S. J. Grabowski and E. Bilewicz, *Chem. Phys. Lett.*, 2006, **427**, 51–55.

48 Y. H. Wang, Y. X. Lu, J. W. Zou and Q. S. Yu, *Int. J. Quantum Chem.*, 2008, **108**, 90–99.

49 Y. X. Lu, J. W. Zou, Y. H. Wang, Y. J. Jiang and Q. S. Yu, *J. Phys. Chem. A*, 2007, **111**, 10781–10788.

50 A. Forni, *J. Phys. Chem. A*, 2009, **113**, 3403–3412.

51 I. Rozas, I. Alkorta and J. Elguero, *J. Am. Chem. Soc.*, 2000, **122**, 11154–11161.

52 J. P. M. Lommers, A. J. Stone, R. Taylor and F. H. Allen, *J. Am. Chem. Soc.*, 1996, **118**, 3108–3116.

53 P. Politzer, P. Lane, M. C. Concha, Y. G. Ma and J. S. Murray, *J. Mol. Model.*, 2007, **13**, 305–311.

54 S. Gowrisankar, H. Neumann, A. Spannenberg and M. Beller, *Acta Crystallogr., Sect. E: Struct. Rep. Online*, 2014, **70**, m255.

55 D. M. L. Goodgame, D. A. Grachvogel, M. A. Hitchman, N. J. Long, H. Stratemeier, A. J. P. White, J. L. M. Wicks and D. Williams, *J. Inorg. Chem.*, 1998, **37**, 6354–6360.

56 A. V. Shtemenko, A. A. Golichenko and K. V. Domasevitch, *Z. Naturforsch., A: Phys. Sci.*, 2001, **56(b)**, 381–385.

57 M. Podsiadlo, K. Dziubek and A. Katrusiak, *Acta Crystallogr., Sect. B: Struct. Sci.*, 2005, **61**, 595–600.

58 O. V. Dolomanov, L. J. Bourhis, R. J. Gildea, J. A. K. Howard and H. Puschmann, *J. Appl. Crystallogr.*, 2009, **42**, 339–341.

59 G. M. Sheldrick, *Acta Crystallogr., Sect. A: Found. Adv.*, 2015, **71**, 3–8.

60 G. M. Sheldrick, *Acta Crystallogr., Sect. A: Found. Crystallogr.*, 2008, **64**, 112–122.

61 A. L. Spek, *PLATON, A Multipurpose Crystallographic Tool*, Utrecht University, Utrecht, The Netherlands, 2005.

62 Bruker, *AXS SAINT*, Bruker AXS, Inc., Madison, WI, USA, 2009.

63 G. M. Sheldrick, *SADABS - Bruker Nonius scaling and absorption correction*, Bruker AXS, Inc., Madison, Wisconsin, USA, 2008.

64 Y. Zhao and D. G. Truhlar, *Theor. Chem. Acc.*, 2008, **120**, 215–241.



65 M. J. Frisch, G. W. Trucks, H. B. Schlegel, G. E. Scuseria, M. A. Robb, J. R. Cheeseman, G. Scalmani, V. Barone, B. Mennucci, G. A. Petersson, H. Nakatsuji, M. Caricato, X. Li, H. P. Hratchian, A. F. Izmaylov, J. Bloino, G. Zheng, J. L. Sonnenberg, M. Hada, M. Ehara, K. Toyota, R. Fukuda, J. Hasegawa, M. Ishida, T. Nakajima, Y. Honda, O. Kitao, H. Nakai, T. Vreven, J. A. Montgomery, Jr., J. E. Peralta, F. Ogliaro, M. Bearpark, J. J. Heyd, E. Brothers, K. N. Kudin, V. N. Staroverov, T. Keith, R. Kobayashi, J. Normand, K. Raghavachari, A. Rendell, J. C. Burant, S. S. Iyengar, J. Tomasi, M. Cossi, N. Rega, J. M. Millam, M. Klene, J. E. Knox, J. B. Cross, V. Bakken, C. Adamo, J. Jaramillo, R. Gomperts, R. E. Stratmann, O. Yazyev, A. J. Austin, R. Cammi, C. Pomelli, J. W. Ochterski, R. L. Martin, K. Morokuma, V. G. Zakrzewski, G. A. Voth, P. Salvador, J. J. Dannenberg, S. Dapprich, A. D. Daniels, O. Farkas, J. B. Foresman, J. V. Ortiz, J. Cioslowski and D. J. Fox, in *Gaussian 09, Revision C.01*, Gaussian, Inc., Wallingford, CT, 2010.

66 D. Andrae, U. Haussermann, M. Dolg, H. Stoll and H. Preuss, *Theor. Chim. Acta*, 1990, 77, 123–141.

67 P. V. Gushchin, M. L. Kuznetsov, Q. Wang, A. A. Karasik, M. Haukka, G. L. Starova and V. Y. Kukushkin, *Dalton Trans.*, 2012, 41, 6922–6931.

68 L. A. Burns, A. Vazquez-Mayagoitia, B. G. Sumpter and C. D. Sherrill, *J. Chem. Phys.*, 2011, 134, 25.

69 M. Sumimoto, Y. Kawashima, D. Yokogawa, K. Hori and H. Fujimoto, *Int. J. Quantum Chem.*, 2013, 113, 272–276.

70 T. Lu and F. W. Chen, *J. Comput. Chem.*, 2012, 33, 580–592.

